Pergamon

Bioorganic & Medicinal Chemistry, Vol. 5, No. 2, pp 353–361, 1997

PII: S0968-0896(96)00254-4
0968-0896/97 $17.00+0.00

Conformational Analysis of the Antimalarial Agent Quinidine

Thais H. A. Silva,[a] Alaíde B. Oliveira[a] and Wagner B. De Almeida[b,*]

[a]*Departamento de Produtos Farmacêuticos, Faculdade de Farmácia da UFMG;* [b]*Laboratório de Química Computacional e Modelagem Molecular (LQC-MM), Departamento de Química, ICEx, UFMG, Belo Horizonte, MG, CEP 31.270-901, Brazil*

Abstract—Quinidine is an active antimalarial compound extracted from the bark of *Cinchona* trees. The activity differences among structurally related molecules appears to depend on the absolute stereochemistry of some functional groups, a result that stimulated a detailed conformational analysis of these molecules of biological interest. In the present study, the potential energy surface (PES) for the antimalarial agent quinidine ($C_{20}H_{24}O_2N_2$) has been comprehensively investigated using the molecular mechanics (MM) and quantum mechanical semiempirical AM1 and PM3 methods. Six distinct minimum energy conformations were located on the multidimensional PES and also characterized as true minima through harmonic frequency analysis. The relative stabilities and thermodynamic properties are reported. The coexistence of different conformers is discussed for the first time in the literature based on the transition state (TS) structures located on the PES for the quinidine molecule. The theoretical results reported in the present study are in agreement with the experimental proposal, based on NMR data, that there are two conformations existing in solution for the quinidine molecule.

Introduction

Quinidine (**1**) is one of the antimalarial constituents of the bark of *Cinchona* trees. It is also used as a cardiac antiarrythmic.[1] Another interesting use of this compound is as a chiral catalyst in asymmetric Michael additions.[2]

Quinine **2** and quinidine **1** (Fig. 1) are a pair of *erythro* diastereoisomers that are active antimalarials. Their *threo* epimers, epiquinine (**3**) and epiquinidine (**4**) (Fig. 1) are practically inactive.[3] As the activity differences appear to depend upon the absolute stereochemistry of their amine and hydroxyl groups, a conformational analysis of the *Cinchona* alkaloids is certainly of interest, and may elucidate important structural characteristics for the antimalarial activity.[4]

Several studies on the structure and conformation of the *Cinchona* alkaloids have already been reported. Prelog and Wihelm in 1954[5] proposed a configuration for the *Cinchona* alkaloids, and ^{1}H NMR data were also used in some conformational studies of these alkaloids.[2,6–8] Conformational analysis studies, using molecular mechanics (MM) and semiempirical methods, have been described.[7,9] The results of the crystal structure analysis for the quinidine[10,11] and quinidine sulfate dihydrate[12] have also been reported. In the theoretical studies reported so far the search for minimum energy structures on the potential energy surface (PES) was not fully carried out, with only three or four local minima being located. Some geometrical constraints were introduced in order to simplify the computational task.

Key words: conformational analysis, antimalarial, quinidine.

In the present study, the PES for the quinidine molecule was comprehensively investigated using MM[13] and the AM1 (Austin Model 1) and PM3 (Parametric Method 3) quantum mechanical semiempirical

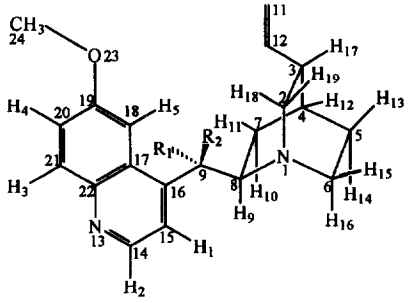

1 and 3

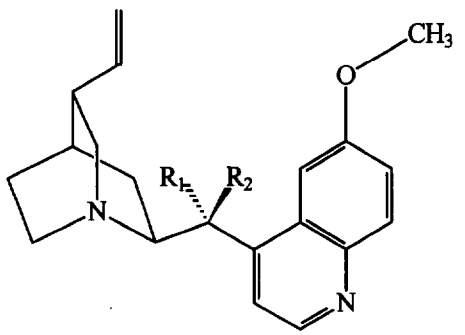

2 and 4

	R_1	R_2
1 and 2	OH	H_8
3 and 4	H_8	OH

Figure 1. The quinidine (**1**), quinine (**2**), epiquinidine (**3**), and epiquinine (**4**) molecules.

methods.[14] The stationary points located on the multidimensional PES were characterized as minima or transition state (TS) structures via harmonic frequencies calculations (for a true minimum energy structure all frequencies must be real). Through this procedure six distinct true minimum energy structures, rather than the three or four reported so far, were found. Previous successful conformational analysis studies for the quinine molecule[15] and other medium sized systems[16–19] carried out in our laboratory give support to the approach adopted here for the conformational analysis of the quinidine molecule. The relative stabilities are reported and the possible coexistence of different isomeric forms discussed. The results of this study are in agreement with the experimental proposal, based on NMR studies, that there are two favored conformations for the quinidine molecule.

It should be said that in the previous theoretical studies on the *Cinchona* alkaloids no assessment on the reliability of the empirical (i.e. MM) and quantum-mechanical semiempirical conformational and energy predictions (including energy barriers) has been made. Also, no attempt to locate precisely TS structures and so evaluate reliable energy barrier values for conformational interconversion has been done.

In this work, for the first time, the conformational interconversion is studied systematically with first order TS structures being located, with the aid of harmonic frequency calculations. We aim to show how an extensively detailed conformational analysis is important for understanding the biological behavior of this class of compounds. It is seen that some important structural features of molecules of biological interest, relevant for structure–activity relationships, may be overlooked if a systematic conformational analysis of the free drug of pharmacological interest is not performed.

Methodology

A comprehensive search for stationary points on the multidimensional PES quinidine ($C_{20}H_{24}O_2N_2$) molecule was carried out using the MM[13] and AM1 and PM3 quantum mechanical semiempirical methods.[14] Thus, a three-dimensional (3-D) PES was constructed by varying the dihedral angles α (N1,C8,C9,C16) and β (C8,C9,C16,C17). A stepsize of 30° was used. For each point on the 3-D PES the remaining geometrical parameters (bond distances, bond angles, and dihedral angles) were fully optimized in the MM calculation. The contour map calculated with the MM method is depicted in Figure 2(A), and the respective isometric projection in Figure 2(C). The 3-D PES was constructed, in a second step, using the quantum mechanical semiempirical PM3 method, which is shown in Figure 2(B) and 2(D) (isometric projections). For reason of simplicity, the bond distances and bond angles were kept unchanged at their optimized values (corresponding to a local minimum), only the remaining dihedral angles were optimized for each calculated point on the 3-D semiempirical surface. By looking at the contour maps a rough geometry of the likely minimum energy structures may be guessed, and by this procedure six minima could be located on both MM and PM3 surfaces. These structures are indicated in Figure 2(A) and 2(B) (labels A–F and 1–6). These stationary points were used as initial guesses for full geometry optimization jobs with the MM2 method (for the stationary points located in the MM surface) and AM1 and PM3 level of theory (for the points located on the semiempirical surface). AM1 and PM3 harmonic frequency calculations were further carried out for the final fully optimized geometries of the stationary points located on the quantum mechanical semiempirical surfaces, aiming to characterize the stationary points as true minimum (all of the eigenvalues of Hessian matrix are positive) or TS structures (occurrence of negative eigenvalues).[20] The Gibbs free energy variations (ΔG) were calculated at the room temperature ($T = 298$ K) using the semiempirical harmonic frequencies to evaluate the entropy (S) contribution according to the well known relation: $\Delta G = \Delta H - T\Delta S$.

The semiempirical calculations were carried out with the MOPAC version 6.0 package,[21] with keywords PRECISE and GNORM = 0.1 being used, as implemented on a SUN SPARC-20 workstation and the MM calculations done with the program PCMODEL version 1.0[13] on a PC AT-486/DX2 microcomputer. All calculations were performed at the Laboratório de Química Computacional e Modelagem Molecular (LQC-MM), Departamento de Química, Universidade Federal de Minas Gerais (UFMG).

Results and Discussion

The quinidine molecule (Fig. 1) consists of two rigid cyclic systems, a heteroaromatic quinoline ring and a quinuclidinic bicyclic system, connected via a carbon atom carrying a hydroxyl group. This molecule posses four asymmetric centers: C3, C4, C8, and C9. Three groups in the molecule are important in the investigation of internal rotation: the vinyl, hydroxyl, and methoxy groups. However, it is the rotation around the C9–C16 and C8–C9 that determine the main conformational changes in the quinidine molecule, since these rotations specify the relative positions of the two rings. The analysis of the MM and PM3 3-D PESs, generated by rotations around the C9–C16 and C8–C9 single bonds, revealed the presence of six distinct minimum energy structures. The structures obtained by direct inspection of the 3-D surfaces were further fully optimized and the geometries, MM energies, heat of formation (ΔH) and Gibbs free energy (ΔG) are given in Table 1. The MM spatial arrangements for the six minima found in the present study are depicted in Figure 3. The experimental values for some dihedral angles and previous theoretical reported values[7,9] and crystallographic structure data[10–12] are also quoted in Table 1, for reason of comparison. The conformations located, respectively, by the MM2, PM3, and AM1 methods are labeled 1–6, A–F, and AA–FF. The

conformations A, B, C, D, E, and F correspond approximately to AA, BB, CC, DD, EE, and FF and to 1, 2, 3, 4, 5, and 6, respectively (Table 1). There is a small difference between the conformations 3 and C (CC) regarding the β angle.

The quinidine molecule forms a diastereoisomeric pair with quinine, but as they differ only about the configurations of the C8 and C9, they are considered 'pseudoenantiomers'.[2] The contour maps of quinidine (Fig. 2) and quinine, previously described,[15] can be considered enantiomorphous because they form mirror images.

The Newman projections in relation to the C8–C9 and C9–C16 bonds for the quinidine conformers are depicted in Figures 4 and 5. Similar to the quinine molecule,[15] three types of rotamers alternated with respect to the C8–C9 bond, were observed (Fig. 4). As was expected, the most stable conformations are the ones where the hydrogens H_8 and H_9 are in antiperiplanar position (conformers A, AA, 1, D, DD, and 4; Fig. 4A). It would be expected that the conformations where the quinolinic ring is overlapped with quinuclidinic ring (Fig. 4C) would exhibit higher energy values. This is verified for the conformers B and E in PM3 calculations, which have higher ΔH values. The same was not observed for the AM1 and MM conformers, where both conformations that have H_8 and H_9 hydrogens in synclinal position are higher in energy (EE, FF, 5, and 6; Fig. 4B, C).

By analyzing the Newman projections with respect to the C9–C16 bond two kinds of alternated rotamers were observed, where the hydroxyl and H_8 atom are on the same side but in opposite side to the quinuclidinic ring, in relation to the plane of the quinolinic ring. (Fig. 5A, B). These conformations are observed for the conformers B, BB, 2, 3, E, EE, 5, F, FF, and 6. Beside these alternated rotamers, two other near-eclipsed ones were found for the conformers C, CC, A, AA, 1, D, DD, and 4 (Fig. 5C, D). Like the quinine molecule[15] the lowest energy conformers have the hydrogen atom H_8 directed to the internal side of the quinolinic ring

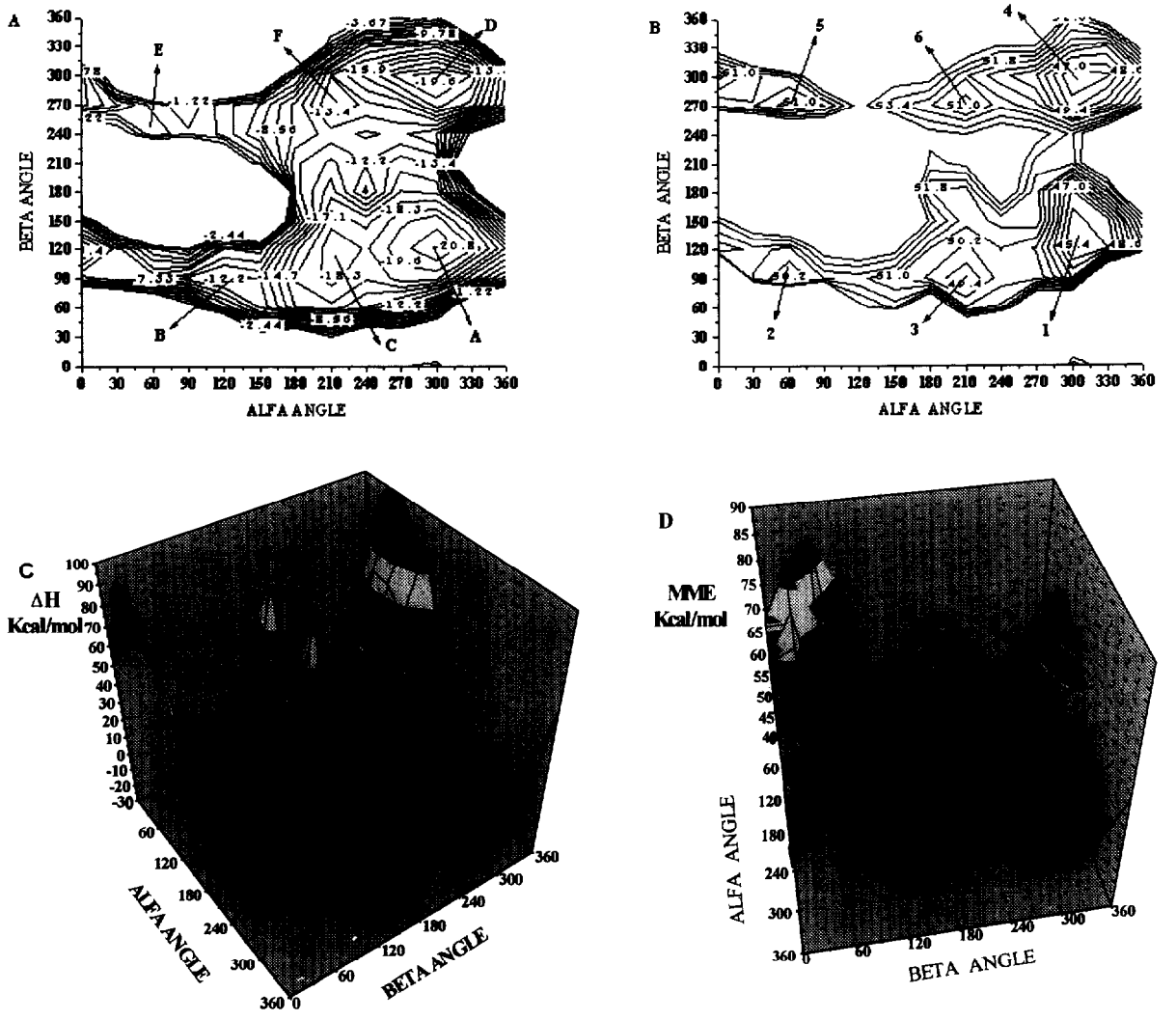

Figure 2. (A) PM3 contour map of the 3-D PES for the quinidine molecule generated by rotations through the α [N1, C8, C9 and C16] and β [C8, C9, C16, and C17] torsion angles. The located minima are indicated by arrows. (B) The MM2 contour map. (C) PM3 isometric projection of the PES for the quinidine molecule. (D) The MM2 isometric projection.

(towards C17), avoiding the steric compression between the hydroxyl and H_5 atom of the quinolinic ring of the other conformations. Then the conformer B (BB and 2, Fig. 5A) is more stable than the conformer E (EE and 5, Fig. 5B), the conformer A (AA and 1, Fig. 5C) is more stable than D (DD and 4, Fig. 5D) and the conformer C (CC, Fig. 5C; and 3, Fig. 5A) is more stable than F (FF and 6, Fig. 5B).

Dijkstra et al.[7] reported a conformational analysis for the quinidine molecule carried out by rotations around the C8–C9 and C8–C16 bonds, using the molecular mechanics MM2P method. In their study four conformations for the quinidine molecule were found (Table 1). Three of them have about the same MME, and the other one is about 4 kcal mol^{-1} less stable. In another investigation Dijkstra et al.[2] reached the conclusion, based in NMR data, that quinidine adopts an open conformation 3 (corresponding to QD3), but there is a certain conformational freedom or flexibility, that can be attributed to the presence in solution of the closed conformation (corresponding to QD2) in minority proportion. Oleksyn et al.[9] also reported a MM2 conformational analysis study for the quinidine molecule where three minimum energy structures were predicted. Oleksyn et al.[9] also concluded that the crystal structure of the quinidine is assigned to conformation QDB (similar to QD3 reported by Dijkstra et al.), since it is the only one capable of forming hydrogen bonds with the surrounding molecules. They assumed that this is the active conformation of the quinidine molecule (i.e. the one able to interact with the receptor site through intermolecular hydrogen bonding).

Among the six conformations reported in this work (Table 1), four of them correspond to the minima given by Dijkstra,[7] and three correspond to the minima given by Oleksyn.[9] So the conformers 4, 1, 3, and 6, here described, correspond to the conformers QD1, QD2, QD3, and QD4 of Dijkstra, respectively, and the conformers 4, 3, and 1 correspond to QDA, QDB, and QDC of Oleksyn. The two other conformations reported in the present work, not found in previous studies,[7,9] are those that have the quinolinic ring overlapped with the quinuclidinic ring (Fig. 4C).

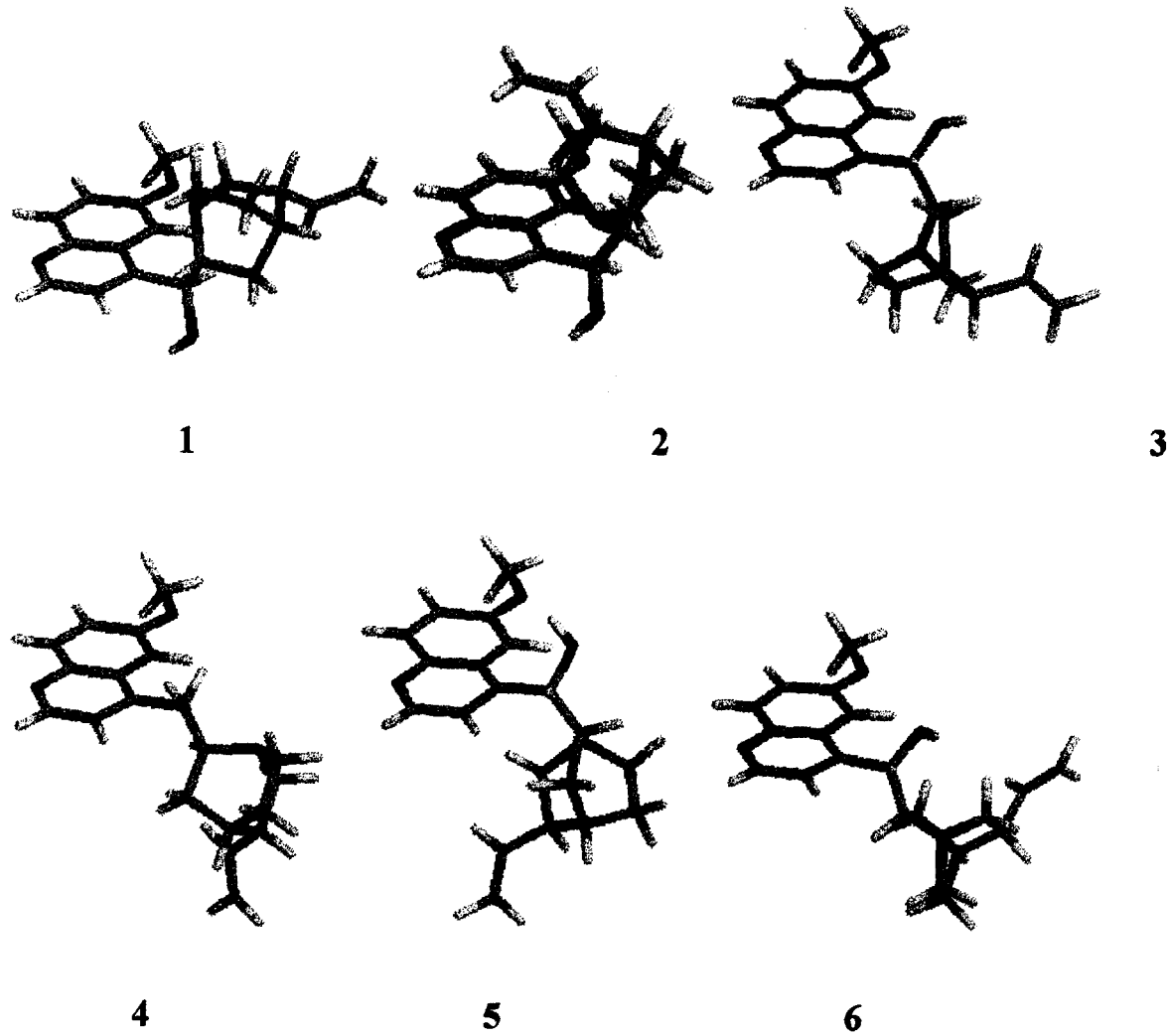

Figure 3. Tridimensional representation of the MM2 fully optimized minimum energy structures located on the PES for the quinidine molecule. The geometric parameters for structures **1–6** are given in Table 1.

Prakash et al.[6] reported a coupling constant (J) value between H_8 and H_9 of 4.6 Hz for the quinidine molecule in $CDCl_3$ solution, which is the same as reported for the quinine molecule. This value corresponds, according to the Karplus–Conroy correlation, to a H_8C9C8H_9 angle of *ca* 80–90°. A similar angle value is predicted in the present work for the conformers B, C, E, and F (and also BB, CC, EE, FF, and 2, 3, 5, 6; Fig. 4B, C and Table 1). Based in the NMR data[6,8] and analyzing the dihedral angles and distances between some protons it may be concluded that the conformer 3 is expected to be the predominant form of the quinidine molecule in solution. This conformation is similar to QD3 (Dijkstra) and QDB (Oleksyn), as was expected. However, the conformation 3 is not the most stable in the gas phase (Table 1).

Table 1. Structural data (dihedral angles in degrees), energies (in kcal mol^{-1}), and thermodynamic properties (in kcal mol^{-1}) of the six conformers located on the PES for the quinidine molecule and for the crystallographic structure[10–12] and previous reported data[7,9]

Conformation	Dihedral angles											
	N1C8 C9C16	C8C9 C16C17	C15C1 6C9C8	O12C9 C16C15	O12C9 C8C7	H8C9 C8H9	C24O2 3C19C18	C11C1 0C3C4	HO12 C9C16			
	PM3 method									*HF*	*ΔHF*	*ΔG*
A	−66.2	124.4	−56.4	69.0	46.9	172.9	179.0	−135.4	−59.0	−21.65	0.0	−68.1
B	89.4	99.1	−84.3	47.1	−169.8	−37.7	177.3	−134.1	−77.9	−18.4	3.3	−63.5
C	−147.2	120.7	−62.9	65.9	−38.0	87.9	178.7	−138.3	−74.5	−20.7	1.0	−66.0
D	−62.1	−65.5	115.1	−118.6	49.75	176.6	−179.5	−135.2	−62.1	−21.3	0.4	−66.2
E	59.1	−98.5	−85.0	−142.5	157.9	−66.9	−179.6	−130.6	−72.3	−16.51	5.1	−61.1
F	−149.7	−85.7	95.1	−133.4	−44.7	82.4	−177.2	−130.6	−84.8	−19.49	2.2	−63.5
	AM1 method											
AA	−54.6	120.0	−60.1	61.7	56.4	−172.8	179.5	−112.2	−56.0	−10.67	0.0	−56.1
BB	59.8	96.4	−87.5	38.9	162.1	−62.8	177.2	−116.4	−73.0	−9.46	1.2	−54.0
CC	−147.3	117.4	−64.7	61.8	−39.7	89.1	179.9	−106.4	−44.8	−9.88	0.8	−55.2
DD	−55.88	−66.9	113.1	−120.8	51.0	−177.9	179.9	−114.0	−49.9	−9.94	0.7	−55.1
EE	56.1	−89.2	95.7	−133.2	154.7	−69.2	179.9	−110.2	−82.2	−6.30	4.4	−51.2
FF	−158.7	−99.4	80.1	−149.5	−56.6	71.5	−173.5	167.0	−102.4	−7.35	3.3	−51.6
	MM2 method									**MME**	**ΔMME**	–
1	−55.0	118.4	−64.2	56.7	−176.5	−172.6	−178.8	−101.9	33.9	45.29	0.0	–
2	52.4	98.3	−84.6	39.5	158.3	−67.3	177.1	167.5	40.5	48.07	2.8	–
3	−154.0	88.8	−91.8	33.9	−46.6	80.6	−180.0	−179.2	43.1	46.37	1.1	–
4	−54.0	−68.8	111.5	−124.1	55.2	−175.6	178.7	−96.2	37.3	45.40	0.1	–
5	55.1	−92.4	90.6	−139.9	155.8	−69.5	172.8	−97.6	30.0	49.11	3.8	–
6	−151.9	−91.5	86.3	−141.4	134.0	77.1	−179.7	175.6	−97.6	50.12	4.8	–
	Quinidine crystallographic structure[10]											
XR1	−162.0	77.8	−100.6	22.1	−47.8	–	−6.3	−79.9	–	–	–	–
	Quinidine crystallographic structure[11]											
XR2	−156.8	52.4	−99.3	13.5	−38.7	–	179.0	−140.0	–	–	–	–
	Quinidine sulfate crystallographic structure[12]											
XR3	−179	74	−103	15	−62	–	6	−115	–	–	–	–
XR4	−158	76	−102	21	−42	–	−3	141	–	–	–	–
	Oleksyn conformers[9]											
QDA	–	–	–	−130	60	–	–	–	–	–	–	–
QDB	–	–	–	25	−52	–	–	–	–	–	–	–
QDC	–	–		57	60	–	–	–	–	–	–	–
	Dijkstra conformers[7]									**MME**	**ΔMME**	
QD1	−53.4	–	104.5	–	–	–	–	–	–	25.5	0.4	–
QD2	−56.6	–	−71.7	–	–	–	–	–	–	25.8	0.6	–
QD3	−156.4	–	−93.8	–	–	–	–	–	–	25.2	0.0	
QD4	178.6	–	84.4	–	–	–	–	–	–	29.2	4.0	–

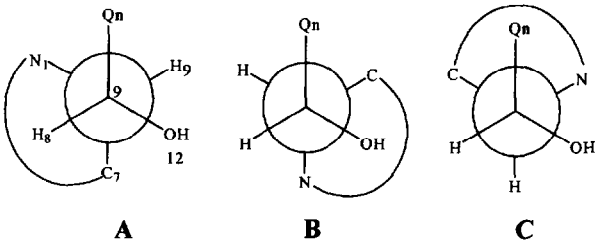

Figure 4. Newman projections with respect to the C8–C9 bond for the quinidine molecule.

Three groups in the quinidine molecule (i.e. vinyl, hydroxyl, and methoxyl groups) appear to posses free rotation around single bonds, based on chemical intuition grounds. The variation of the MME energy due to rotations of these groups around single bonds was calculated for the conformer 3 with a stepsize of 10°, and optimizing all the remaining geometrical parameters for each point. The resulting potential energy curves are shown in Figure 6.

It can be seen from Figure 6 that the CH_3O- group is able to assume two distinct positions at approximately 180° and 0° in relation to the dihedral angle C24O23C19C18, with a relatively small energy barrier for interconversion of *ca* 3 kcal mol^{-1}. Both angles correspond to the X-ray structures values reported previously[10-12] (Table 1). A very similar rotation curve was observed for the quinine molecule.[15]

The HO- rotation, as shown in Figure 8, is predicted to be practically free. There is a second minimum energy structure of *ca* 2 kcal mol^{-1} above the structure given in Table 1 (HO12C9C16 = −65°), with the energy barrier for interconversion being only 0.5 kcal mol^{-1}. Also a third very shallow minima is seen at an angle of *ca* +135° with a negligible barrier for interconversion of *ca* 0.3 kcal mol^{-1}. This is a very interesting result because the curve of the rotation of the OH angle for

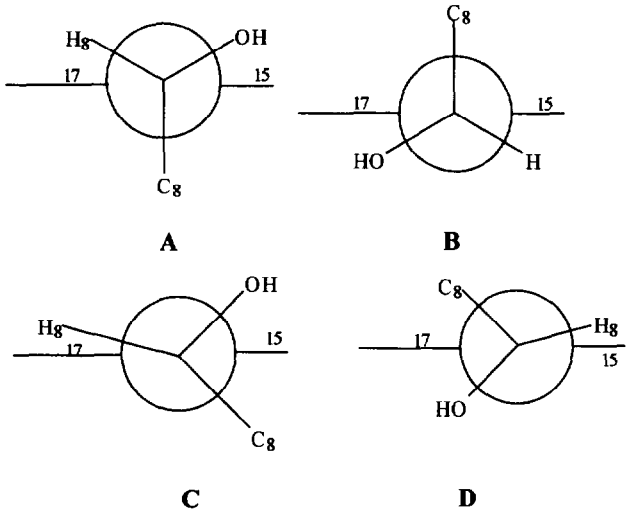

Figure 5. Newman projections with respect to the C9–C16 bond for the quinidine molecule. The horizontal lines represent the quinoline nucleus perpendicular to the paper plane and behind C9.

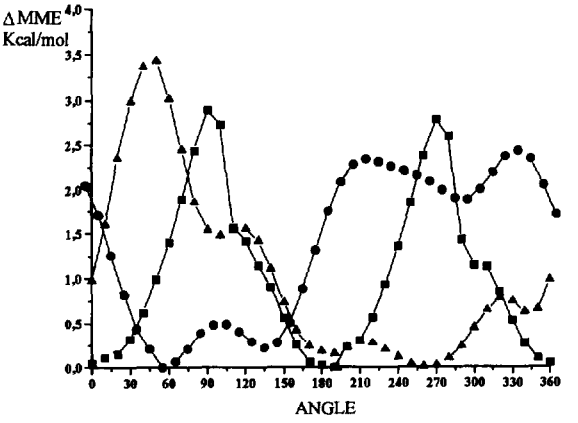

Figure 6. The MM2 pointwise calculated 1-D PES for rotation through the [C24, O23, C19, and C18] angle (methoxy group, square), [H, O12, C9, and C16] angle (hydroxyl group, circle), and [C11, C10, C3, and C4] angle (vinyl group, triangle), using as the starting geometry the conformer 3 and optimizing all the remaining geometrical parameters.

the quinine molecule[15] is a quite mirror image of the curve depicted in Figure 6. It must be remembered that the configurations of the carbons containing the hydroxyl groups are opposite in these two molecules.

The potential energy curve depicted in Figure 6 shows that there are four possible positions relative to the quinuclidinic ring for the vinyl group (i.e. at angles of *ca* −100, −170, −40, and 100°; in increasing energetic order), with small barriers for interconversions, varying between 0.1 to 2 kcal mol^{-1}. The X-ray result for this dihedral angle (Table 1) agree with the lowest energy structure located on the potential energy curve from Figure 6, showing that the preferred orientation of the vinyl group in the gas phase is maintained in the crystal structure. The curve showed in Figure 6 is very similar to the respective one reported for the quinine molecule.[15]

From the contour maps and isometric projections depicted in Figure 2 it can be seen that there are two valleys on the PES parallel to the α angle direction and separated by two high energy regions (hills). This means that the conformational interconversions inside the valleys (i.e. involving conformations that have approximately the same value for the torsion angle β) is easier because the transition state (TS) structure connecting the two minima is of low energy. On the other hand the interconversion through two valleys (i.e. involving a rotation around the β angle) is more hindered because the TS structure must be energetically much higher. So it can be concluded that the interconversions A = B = C = A and D = E = F = D should be the favored ones. Among the lower energy conformations (A, C, D, AA, CC, DD, 1, 3, and 4) the interconversion between conformers 1 (A and AA) and 3 (C and CC) should be more facile because the respective TS structure is of lower energy. From Figure 2 it can be seen that the MM value for this barrier is *ca* 2.2 kcal mol^{-1} and the PM3 value is *ca* 1.1 kcal mol^{-1}.

In order to better understand the plausible conformational interconversions the MM potential energy curves for rotation around α and β torsion angles were constructed, using as the starting configuration the minimum 1 and 4 (Fig. 7) and 1, 2, and 3 (Fig. 8), with all remaining geometrical parameters being fully optimized for each point on the curve. From Figure 7 the energy barriers for the interconversions 2→1, 2→3, 3→1, 5→4, 5→6, and 6→4 are 1.5, 2.5, 2.4, 0.3, 4.4, and 1.6 kcal mol^{-1}, respectively. As the interconversions 2→1, 5→4, and 6→4 have a low energy barrier, there is a negligible probability of the structures 2, 5, and 6 being observed. If a Boltzmann population analysis for these structures in equilibrium is performed it is easy to predict that the three conformers 1, 3, and 4 will have a significant probability of coexistence.

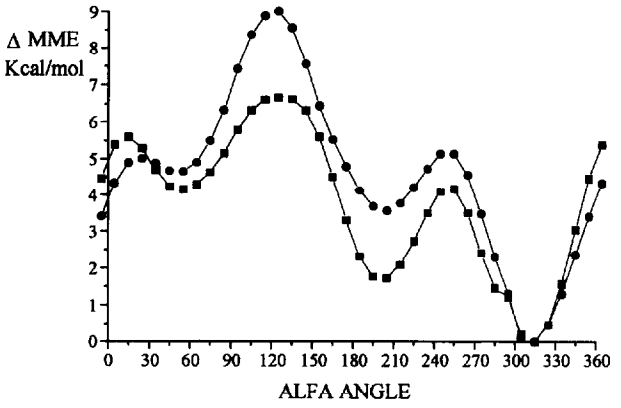

Figure 7. One-dimensional representation of the MM PES for the quinidine molecule generated by rotation through the α [N1, C8, C9, and C16] angle, using as the starting geometry the conformers 1 (square) and 4 (circle). All remaining geometrical parameters were fully optimized for each point on the potential energy curve.

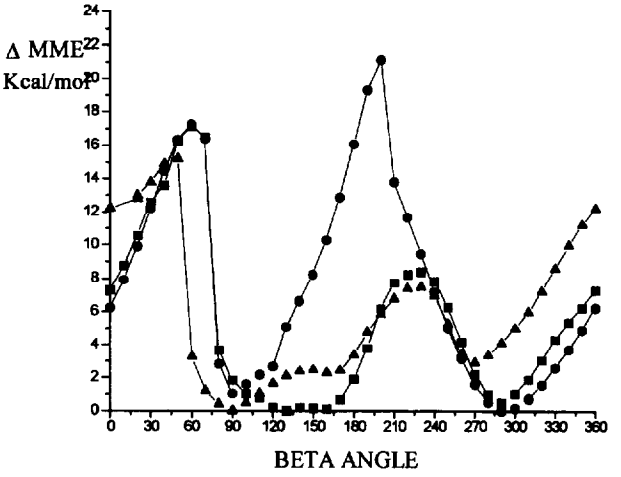

Figure 8. One-dimensional representation of the MM PES for the quinidine molecule generated by rotation through the β [C8, C9, C16, and C17] angle, using as the starting geometry the conformers 1 (square), 2 (circle), and 3 (triangle). All remaining geometrical parameters were fully optimized for each point on the potential energy curve.

An approximated TS structure located on the PM3 PES (Fig. 2) connecting the conformers A and C (i.e. $\alpha = -120°$ and $\beta = 120°$) had its remaining geometrical parameters fully optimized and the final geometry for the TS showed a ΔH value of -18.9 kcal mol^{-1}. With this value the energy barrier was estimated as 2.5 kcal mol^{-1}. By fully optimizing the geometry of this trial TS structure, using an option for locating points on the negative curvature of the PES, and further performing harmonic frequency analysis, a first-order TS structure (having only one negative eigenvalue of the Hessian matrix) was located. The final dihedral angles are $\alpha = -112.7$ and $\beta = 115.2$ and the heat of formation -18.9 kcal mol^{-1}. The correct PM3 energy barrier for the interconversion between conformers A and C, with the respective TS structure (TS_{AC}) depicted in Figure 9, evaluated as the energy difference between the fully optimized TS structure and the respective minimum, is predicted to be 1.8 kcal mol^{-1}.

From the calculated potential energy curves for β angle rotation (Fig. 8) the barriers (h in kcal mol^{-1}) for the following conformational interconversions were respectively: 4↔1 (h = 7.9 and 16.7), 2↔5 (h = 15.7 and 19.6) and 6↔3 (h = 4.6 and 12.3). It can be seem that the 4↔1 interconversion has an energy barrier approximately two to four times higher than the respective value for the 1↔3 process. So the 1↔3 interconversion is significantly more favored than the 1↔4 one. Therefore, there is a great probability of the coexistence, in the gaseous phase, of the conformers 1 and 3.

The results presented in the last sections are in agreement with the proposal of Dijkstra et al.,[2] based on the ^1H NMR data, that in solution there is a certain conformational freedom or structural flexibility and then QD3 (majority), and QD1 (minority) may coexist. It should be remembered that QD3 and QD1 are, respectively, equivalent to the 3,C,CC and 1,A,AA conformers reported in the present work. In the gas phase, the conformations 1, 4, and 3 show the lowest MME values. The factors that drive the conformer 3 to be the majority in solution can be assumed to be the easier 1↔3 interconversion compared with the 1↔4 one and that, in solution, the conformer 3 is the only one that can form hydrogen bonds with the surrounding molecules.

A similar result was found for the quinine molecule, where it was demonstrated that there is an conformational equilibrium and that the interconversion takes place via rotation of the α angle.[15] When the conformers of the two molecules involved in these interconversions are superimposed, it can be seem that they are mirror images. Then the aliphatic nitrogen and the oxygen atoms are turn to the same side in relation of the position of the quinolinic ring. For a comparison see the Newman projections for the conformer D of quinine[15] and C of quinidine given in Figure 10.

Table 2 shows the quinuclidinic bridged system dihedral angles for the PM3, AM1, and MM conformers

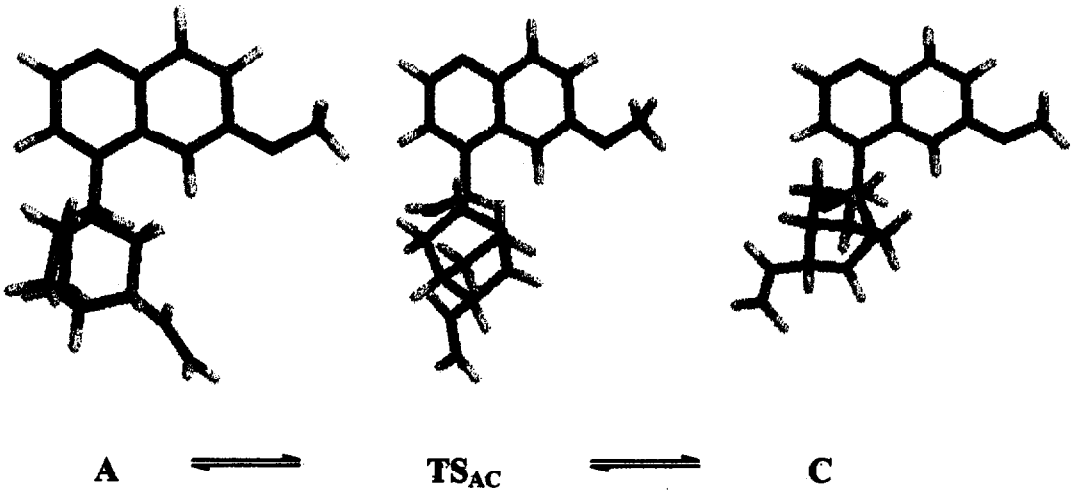

Figure 9. Pictorial representation of a conformation interconversion between conformers A and C, on the PM3 PES for the quinine molecule, through a first-order transition state structure TS_{AC}.

and for the reported crystalline structures of quinidine[10,11] (XR1 and XR2) and the quinidine sulfate[12] (XR3 and XR4). The respective angles found by the analysis of the coupled constants of the (*p*-chlorobenzoyl)dihydroquinidine (NMR1) in toluene-d_8 solution[8] are also given. By looking at Table 2, it can be verified that the crystal structures of the quinidine (XR1 and XR2) and of the quinidine sulfate (XR3 and XR4) show a torsion in a bridged system smaller than of the (*p*-chlorobenzoyl)dihydroquinidine in solution (NMR1). In the gas phase there is a great variety of torsion angles for the quinuclidinic ring. For the conformer 3 (C,CC) these torsion angles are smaller than the crystal structures of the quinidine (XR1 and XR2) and the quinidine sulfate (XR3 and XR4).

Finally, it should be said that in the present work a clear explanation, based on the following reasons, is given for the previous suggestion that there are two isomers of the quinidine molecule in equilibrium (1↔3): (i) this is a significant lower energy barrier conformational interconversion process than the 1↔4 one; (ii) also the mechanism of interconversion is demonstrated to take place via a rotation of a single bond, (i.e. through the α torsion angle, Fig. 7); and (iii) the interconversion through the torsion β angle involves a barrier three times higher. The next step regarding the theoretical investigation of the quinidine and structurally related molecules is the consideration of solvent effects on the conformation equilibrium and molecular properties.

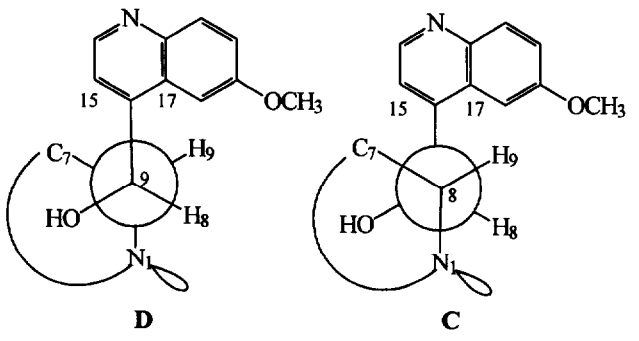

Figure 10. The Newman projection of the conformers D of the quinine[15] and C of the quinidine.

Table 2. Semiempirical, MM and X-ray dihedral angles (°) of the quinuclidinic ring for the six conformers of the quinidine molecule for the crystallographic structures of quinidine (XR1[10] and XR2[11]) and the quinidine sulfate dihydrate (XR3[12] and for the of *p*-cloro-benzoyldihydroquinidine in solution, NMR1[8]).

Conformation	Dihedral angles					
	N1C8 C7C4	C4C5 C6N1	N1C2 C3C4	C7C4 N1C8	C5C4 N1C6	C3C4 N1C2
A	8.1	5.3	7.2	4.9	3.2	4.3
B	14.7	8.2	7.5	8.9	4.9	4.5
C	10.5	6.3	7.7	6.3	3.8	4.6
D	7.2	4.7	6.7	4.4	2.8	4.1
E	15.3	8.9	8.4	9.2	5.3	5.1
F	6.1	2.7	2.3	3.7	1.6	1.4
AA	4.1	2.5	4.3	2.5	1.5	2.6
BB	18.0	12.2	13.6	10.7	7.2	8.1
CC	6.2	4.7	7.3	3.7	2.8	4.3
DD	5.2	3.2	4.8	3.1	1.9	2.8
EE	15.9	10.4	11.2	9.5	6.2	6.6
FF	4.1	1.7	2.1	2.4	1.0	1.3
1	7.3	7.4	6.2	4.4	4.5	3.8
2	23.3	17.8	18.5	14.1	10.8	11.2
3	7.9	8.6	7.4	5.2	5.5	4.6
4	10.6	10.1	8.9	6.4	6.1	5.4
5	21.7	17.8	19.4	13.2	10.8	11.8
6	13.5	13.0	11.9	8.1	7.8	7.2
XR-1	13.7	9.7	14.4	8.9	7.4	6.9
XR-2	16.3	13.0	9.7	10	8	5
XR-3	17.4	16.9	14.5	11	10	9
XR-4	20.4	18.6	18.4	13	11	12
NMR1	25	20	20	–	–	–

Acknowledgment

W. B. De Almeida would like to thank the Conselho Nacional de Desenvolvimento Científico e Tecnológico (CNPq) for support. This project has been sponsored by the PADCT-II program (Project No. 62.0241/95.0). The authors would like to acknowledge this CNPq/PADCT support.

References

1. Korolkovas, A. *Essęntials of Medicinal Chemistry*; Wiley-Interscience: New York, 1988.

2. Dijkstra, G. D. H.; Kellogg, R. M.; Wynberg, H. *J. Org. Chem.* **1990**, *55*, 6121.

3. Karle, J. M; Karle, I. L.; Gerena, L.; Milhous, W. K. *Antimicrobial Ag. Chemother.* **1992**, *36*, 1538.

4. Karle, J. M.; Olmeda, R.; Gerena, L. ; Milhous, W. K. *Exp. Parasitol.* **1993**, *76*, 345.

5. Prelog, U.; Wilhelm, M. *Helv. Chim. Acta* **1954**, *37*, 1634.

6. Prakash, O.; Roy, R.; Singh, I.; Pratap, R.; Popli, S. P.; Bhakuni, D. S. *Indian J. Chem.* **1988**, *27B*, 950.

7. Dijkstra, G. D. H.; Kellogg, R. M.; Wynberg, H. *Recuel Travaux Pays-Bas* **1989**, *108*, 195.

8. Dijkstra, G. D. H.; Kellogg, R. M.; Wynberg, H.; Svendsen, I. M.; Sharpless, K. B. *J. Am. Chem. Soc.* **1989**, *111*, 8069.

9. Oleksyn, B. J.; Suszko-Purzycka, A.; Dive, G.; Lamotte-Brasseur, J. *J. Pharm. Sci.* **1992**, *81*, 122.

10. Doherty, R.; Benson, W. R.; Maienthal, M.; Stewart, J. M. *J. Pharm. Sci.* **1978**, *67*, 1698.

11. Kashino, S.; Haisa, M. *Acta Cryst.* **1983**, *C39*, 310.

12. Karle, J.; Karle, J. *Proc. Natl. Acad. Sci. U.S.A.* **1981**, *78*, 5938.

13. PCMODEL 1993 Serena Software—First edition. The force field used in PCMODEL is called MMX and is derived from MM2 (QCPE-395,1977) force field of N. L. Allinger, with the pi-VESCF routines taken from MMP1 (QPCE-318), also by N. L. Allinger.

14. (a) AM1: Dewar, M. J. S.; Zoebisch, E. G.; Healy, E. F.; Stewart, J. J. P. *J. Am. Chem. Soc.* **1985**, *107*, 3902. (b) PM3: Stewart, J. J. P. *J. Comput. Chem.* **1989**, *10*, 209.

15. Silva, T. H. A.; Oliveira, A. B.; De Almeida, W. B. *Struct. Chem.* **1996**, in press.

16. Dos Santos, H. F.; Taylor-Gomes, J.; Booth, B. L.; De Almeida, W. B. *Vibrat. Spectrosc.* **1995**, *10*, 13.

17. De Almeida, W. B.; Dos Santos, H. F.; O'Malley, P. J. *Struct. Chem.* **1995**, *6*, 383.

18. Do Val, A. M. G.; Guimarães, A. C.; De Almeida, W. B. *J. Heterocycl. Chem.* **1995**, *32*, 557.

19. Rocha, W. R.; De Almeida, W. B. *J. Comput. Chem.* **1996**, in press.

20. Mezey. P. G. *Studies in Physical and Theoretical Chemistry: Potential Energy Hypersurfaces*; Elsevier: Amsterdan, Vol. 53, 1987.

21. MOPAC version 6.0, J. J. P. Stewart, Frank J. Seiler Research Laboratory, US Air Force Academy, Colorado Springs, CO, 1990.

(*Received in U.S.A.* 26 *July* 1996; *accepted* 19 *September* 1996)